

# Intercalating Cationic Surfactants in Koppies Bentonite

**Running title:** Intercalating Cationic Surfactants in Koppies Bentonite

**Pedro H. Massinga Jr.<sup>1</sup>, Walter W. Focke**

Institute of Applied Materials, Department of Chemical Engineering, University of Pretoria, Pretoria 0002, South Africa

## **Abstract**

Single and double chain cationic surfactants were intercalated into Koppies bentonite. The state of the chains in the interlayers was probed using XRD, FTIR spectroscopy and thermogravimetric analysis (TG). The degree of intercalation was determined by TG and exceeded the CEC equivalent value by 30-40 %. The degradation onset temperature of about 200 °C was independent of the number and length of alkyl chain substituents. The XRD d-spacing was consistent with monolayer interdigitated surfactant intercalation for the C12 and C14 single chain surfactants and with bilayer intercalation of the double chain surfactants. FTIR analysis revealed disordered alkyl chain conformations.

**Keywords:** bentonite, alkylammonium, intercalation, basal spacing, conformations, thermal stability.

---

<sup>1</sup> Corresponding Author: Universidade Eduardo Mondlane; Faculdade de Ciências; Campus Universitário Principal; Av. Julius Nyerere; P.O. Box 257; Maputo, Moçambique; E-mail: massingajr@uem.mz

## Introduction

Organoclays include the class of clay minerals intercalated with quaternary alkylammonium surfactants. They have attracted attention as functional additives that enhance desirable properties of polymeric materials. The thermal stability of organoclays and their basal or d-spacing ( $d_{001}$ ) both affect the preparation and performance of clay-polymer composites. Higher d-spacings facilitate delamination and dispersion of organoclay particles in a polymer matrix. Lower degradation onset temperatures limit the processing temperatures of the nanocomposites.

The effect of alkyl chain length and surfactant loading on the d-spacing of organoclays, as well as the arrangement and state of the intercalated surfactants have been the subject of numerous investigations [1]. It is well known that the d-spacing increases with increasing surfactant loading. The loading may exceed the cation exchange capacity (CEC) of the clay mineral. The maximum d-spacing is realized at a certain critical surfactant loading, beyond which no further expansion occurs [1]. This critical surfactant loading depends on the clay CEC. At the critical surfactant loading, its alkyl chain length influences the maximum d-spacing [2]. Increasing the chain length tends to increase the maximum d-spacing. Ultimately, it is the surfactant conformation, rather than its amount intercalated or its chain length what essentially determines the d-spacing that can be achieved [2]. This does not detract from the roles that the amount of surfactant intercalated and its chain length plays with regard to the d-spacing.

The thermogravimetric decomposition onset temperature  $T_{\text{onset}}$  provides an indicator for thermal stability of organoclays. A previous study concluded that different lengths of quaternary alkylammonium surfactants have no effects or very little effect on the thermal decomposition of organoclays [3]. Current study investigated the effect of the number of substituents of quaternary alkylammonium surfactants on the thermal decomposition of

organoclays. Additionally, it examined the influence of the number and length of the long-chain alkyl substituents of the surfactant on the nature and amount of surfactant intercalated. Towards these purposes, Koppies bentonite was intercalated with cationic quaternary ammonium surfactants. Surfactants with single or double alkyl chain substituents, and with different chain lengths, were used. The expansion of the basal spacing was followed to confirm that intercalation indeed occurred. The thermal stability of resultant organobentonites and the degree of intercalation was estimated from thermogravimetric data. The nature of the chains in the interlayer was probed via FTIR.

## **Materials and Methods**

### *Materials*

G & W Base and Industrial Minerals supplied bentonite samples mined at Koppies in South Africa. The dry powder (KP) consisted of the neat mined clay in a finely milled form. The water-based slurry sample (KS) was a sodium carbonate activated Koppies bentonite purified by proprietary centrifugation and sedimentation processes. The KS slurry had a light brown colour, a pH of 9.9 and a solid content of 18.9 % by mass. The cation exchange capacity (CEC) was determined by the supplier using the methylene blue method [4] and was stated to be 0.85 meq/g of dry clay.

Quaternary ammonium surfactants (Quats) with single and double alkyl chains were utilised as supplied. The single chain quats comprised the following number of carbon atoms (C): 12 (lauryl dimethyl hydroxyethylammonium chloride, ex Huntsman Surface Sciences UK) and 14 (tetradecyltrimethylammonium bromide – Cetrinide BP, Purum grade, ex FeF Chemicals A/S, Copenhagen). The single chain C12 was supplied in its isopropanol solution, while the C14 was supplied in powder form. The double chain quats comprised C10 (N,N'-didecyldimethylammonium chloride, i.e. M21080 supplied by CECA – ARKEMA Group), C16 (Varisoft 432 CG, a product of Degussa – Goldschmidt GmbH that contains mostly

N,N'-dihexadecyldimethylammonium chloride) and C18 (N,N'-dihydrogenated tallow dimethylammonium chloride, M2SH-1, a product of CECA – ARKEMA Group). The latter is a mixture of alkyl chain homologs with 64% C18 (saturated), 35% C16 (saturated) and 1% C18 (double bond). The composition is given in mass percent. All double chain quats were supplied and used as isopropanol solutions.

### ***Intercalation***

Intercalation experiments were conducted as reported in our previous communication [5]. A mass of quat corresponding to 1.5 times the equivalent of the bentonite CEC (i.e. an excess of 50%) was used in each experiment. The organoclays synthesized in the scope of this work were coded SCXX or DCXX where SC and DC indicate single chain and double chains respectively, while XX represents the number of carbon atoms in each alkyl chain.

### ***Characterization***

X-ray diffraction (XRD), Fourier transform infrared (FTIR) spectroscopy, thermogravimetric (TG) analysis and X-ray fluorescence (XRF) were used to characterize the samples before and after organic treatment. XRD mineral identification and composition assessment of pristine bentonite was performed on oriented and randomly oriented samples by the South African Council for Geoscience. The XRD instrument used was a BRUKER D8 Advance diffractometer using Cu K $\alpha$  radiation ( $\lambda = 0.15406$  nm). The system featured a Johansson crystal primary monochromator and LynxEye detector with 3.7 ° active area. XRD patterns were recorded for random powder preparations. The mineral identification was based on a BRUKER DIFFRACPlus – EVA evaluation program. The phase concentrations were determined by Rietveld quantitative analysis with DIFFRACPlus – TOPAS software to an accuracy of  $\pm 1$  %. In turn, the basal spacing values were also determined in-house, using a PANalytical X-pert Pro powder diffractometer. The instrument featured variable divergence

and receiving slits and an X'celerator detector using Fe filtered Co K $\alpha$  radiation ( $\lambda=0.17901$  nm). XRD analyses were performed on randomised powder samples. X'Pert High Score Plus software was used for data reduction. FTIR spectra were recorded on a Perkin Elmer RX I spectrometer. Approximately 2 mg of dry sample was combined with 100 mg of spectroscopic grade KBr and ground into a fine powder. The mixture was pressed into a 13 mm  $\phi$  die pellet. The reported spectra represent averages of 32 scans at a resolution of 2 cm<sup>-1</sup>. The averaged data was background-corrected using a pure KBr pellet. Thermal analysis was performed using the dynamic method on a Mettler Toledo A851 TGA/SDTA instrument. About 15 mg powder was placed in open 70  $\mu$ L alumina pans. Temperature was scanned from 25 to 1000 °C at a rate of 10 °C/min with air flowing at a rate of 50 mL/min. Elemental composition was determined by XRF. The intercalated materials were ashed before analysis in order to reduce their bulk. The samples were ground to < 75  $\mu$ m in a tungsten carbide mill and roasted at 1000°C. Then 1 g sample was added to 9 g Li<sub>2</sub>B<sub>4</sub>O<sub>7</sub> and fused into a glassed bead. Major element analysis was executed on the fused bead using an ARL9400XP+ spectrometer.

## Results and Discussion

The chemical composition of the Koppies clay is presented in Table 1. The Rietveld quantitative analysis of the pristine Koppies bentonite XRD data indicated the following composition, in mass percent: 38.86% dioctahedral smectite (montmorillonite), 26.68% quartz, 11.14% plagioclase, kaolinite and K-feldspar 10.42% each, 1.51% mica and about 1% calcite. The montmorillonite phase was identified by the  $d_{001} = 1.50$  nm coupled with  $d_{060} = 0.15$  nm and the Greene-Kelly test. The test consisted of Li-saturation, glycolation and heating to 300 °C. After this treatment, the basal spacing collapsed to 0.96 nm indicating montmorillonite [6]. Upon

ethylene glycol saturation for 24 h, the  $d_{001}$  expanded to 1.72 nm and collapsed to 1.03 nm after heating for 1 h at 550 °C [7].

### ***Basal spacing expansion and arrangements of the intercalated surfactants***

XRD patterns of crude bentonite KP and the organic derivatives are presented in Figure 1. KP shows a basal reflection of MMT at  $2\theta = 6.763^\circ$ , corresponding to  $d_{001} = 1.52$  nm. It is within the 1.2-1.6 nm, the range of values for typical smectite minerals under ambient temperature and humidity conditions [8]. The changes in the observed d-spacings indicate that the surfactants were successfully intercalated into the clay. The d-spacing of the organobentonites increased relative to that of pristine KP (Table 2) as indicated by the shift in  $2\theta$  to lower values (Figure 1).

The physical arrangements of the alkyl chains of intercalated quaternary ammonium species (quats) have been the subject of intense debate [9–11]. At high surfactant loadings, two limiting cases are envisioned. One assumes that the chains are present as tilted extended chain paraffin-like arrangements. The alternative assumes disordered chain conformations containing numerous gauche conformers [9]. These two different arrangements, although indistinguishable by XRD, nevertheless constitute very different molecular environments and interlayer structures [11]. The d-spacing values observed for the present organobentonites are consistent with both options.

When the alkyl groups of intercalated surfactants adopt paraffin-like chain extended conformations, they tilt at an angle  $\alpha$  with respect to the plane of the clay mineral layers for yielding a space-filled packing [10, 12–15]. The expected basal spacing values are then given by the following approximate expressions [15, 16]:

$$\text{Interdigitated monolayer:} \quad d_L = 1.18 + 0.127 n_C \sin \alpha \quad (1)$$

$$\text{Bilayer:} \quad d_L = 1.66 + 0.254 n_C \sin \alpha \quad (2)$$

Where  $d_L$  is the basal spacing,  $n_C$  is the number of carbon atoms in the alkyl chain and  $\alpha$  is the tilt angle. The values indicated for the constants in these equations are only approximate. They take into account the following contributions [14, 15]: the thickness of the bentonite layer (0.66 nm); the van der Waals radius of surface oxygen atoms (0.14 nm); the van der Waals radius of a methyl group (0.20 nm); the distance between a terminal methyl group and an oxygen atom (0.12 nm); the projected length of the C–N bond (0.12 nm); a correction accounting for the fact that methyl groups can actually penetrate the six-member oxygen rings of the silicate sheets (maximum depth 0.13 nm), and finally the gap between the terminal methyl groups for the case of bilayer intercalation (0.20 nm). These values yield separation distances of  $x\text{CH}_3\cdots\text{O} \approx 0.12$  nm and  $x\text{N}-\text{CH}_3\cdots\text{O} \approx 0.40$  nm.

The XRD measured basal spacings are presented in Table 2. The values obtained for single chain surfactant intercalated bentonites are consistent with a monolayer configuration. In turn, the basal spacings of the double chain surfactant intercalated bentonites are consistent with a bilayer configuration. The angle  $\alpha$ , at which the respective alkyl chains tilted with respect to the plane of the clay mineral layers are likewise presented in Table 2. The tilt angles were estimated from the measured basal spacing values using equation (1) or equation (2). The present angles are equivalent to about half the reported value of ca.  $59^\circ$  for typical paraffin-type conformations [10]. This suggests that the chains adopted disordered conformations with numerous gauche conformers [9].

FTIR  $\text{CH}_2$  asymmetric band [ $\nu_{\text{as}}(\text{CH}_2)$ ] can also probe the nature of the interlayer structure [11]. The wavenumber and the width of  $\nu_{\text{as}}(\text{CH}_2)$  are very sensitive to the gauche/trans conformers ratio. The former varies from  $2917.8\text{ cm}^{-1}$  for the methylene chains in the all-trans ordered state, in a crystalline surfactant, to  $2928.9\text{ cm}^{-1}$  when the chains are in a liquid-like environment [11, 12]. The frequencies of  $\nu_{\text{as}}(\text{CH}_2)$  found for present organobentonites are presented in Table 2. For all the surfactants, regardless of the number of

chains, the observed values shifted towards values more consistent with the all-trans ordered state with increase in the alkyl chain lengths. It is speculated, however, that the intercalated alkyl chains did not adopt a rigid solid-like configuration. Instead it is likely that they were mobile while simultaneously maintaining some degree of orientational order reminiscent of a liquid–crystalline state.

### ***Degree of intercalation***

Thermogravimetric analyses (TGA) provides information on the amount of intercalated surfactant [1, 3, 17, 18]. Fig. 2 reports the stepwise TG mass losses recorded for the present organobentonites. As expected, mass loss increased with increasing number of alkyl chain substituents of surfactants. The organic content was estimated from the mass losses between 150 and 1000 °C, relative to the mass loss recorded for the bentonite slurry (Table 3). The values were compared with the organic content calculated on the basis of total ion exchange equivalent to the bentonite CEC. All surfactants used, whether single–tailed or double–tailed, were intercalated in excess of the value equivalent to the CEC value of the bentonite. The single-alkyl-chain surfactants intercalated at ca. 1.1 times the CEC. The double-chain surfactants intercalated at about 1.4 times the CEC. Surfactants intercalated up to the CEC are incorporated as the free cationic species. These cations are electrostatically “attached” to the charged clay surfaces. The surfactants intercalated beyond this level are probably present as their corresponding salts. Their incorporation is driven by the so-called hydrophobic interactions between the alkyl chains.

### ***Thermal stability***

The thermogravimetric decomposition onset temperature  $T_{\text{onset}}$  provides an indicator for thermal stability of organoclays. It is defined as the intercept of the tangents of the initial plateau and that of its main slope on the TG curves [18]. The onset decomposition

temperature of present organobentonites is about 200 °C (Fig. 2) irrespective of the alkyl chain length [3] and number of alkyl chains.

Figure 3 presents derivative TG curves for the present organobentonites. These curves show several peaks indicating that the degradation proceeds in several consecutive steps. These mass loss steps are related to the structure of the inserted molecule [1, 17]. For all the surfactants, most of the mass loss occurred in the same temperature range, i.e. 200–400 °C, regardless of the length or number of alkyl chain substituents. The main decomposition step is tagged by  $T_{\text{peak}}$ , the peak temperature corresponding to the maximum mass loss rate. For single chain intercalated surfactants, only hints of weak peaks were observed below  $T_{\text{peak}}$ . With the double chain surfactants a more pronounced peak was observed below  $T_{\text{peak}}$ . The intensity of the main degradation event ( $T_{\text{peak}}$ ) increased with chain length for single-chain surfactants. Conversely,  $T_{\text{peak}}$  decreased with increasing chain length for double chain surfactants. Similar results for surfactants with two alkyl chain were previously reported [18]. The decrease in  $T_{\text{peak}}$  was attributed to the development of ordered solid-like chain conformations [18]. However, in this context, the  $T_{\text{peak}}$  trends observed for the present organobentonites are in contradiction to the trends indicated by the downward shift in FTIR  $\nu_{\text{as}}(\text{CH}_2)$ . This suggests that the degradation mechanism of the surfactants might not be as sensitive to the molecular arrangements of the surfactants in the interlayer as has been surmised.

The FTIR  $\text{CH}_2$  bending mode [ $\delta(\text{CH}_2)$ ] reportedly provides useful additional information [11]. A sharp and intense band located around 1472  $\text{cm}^{-1}$  indicates strong interchain interactions. Conversely, band broadening coupled with decrease intensity at a location around 1466  $\text{cm}^{-1}$  reflects reduced interactions between methylene groups on neighbouring chains [11]. The  $\delta(\text{CH}_2)$  wavenumbers found for the present organobentonites are presented in Table 2. Except for SC12 and SC14, the other  $\delta(\text{CH}_2)$  wavenumbers were similar and located in

the middle of the range 1466–1472  $\text{cm}^{-1}$ . As indicated above, the SC12 and SC14 organoclay samples feature interdigitated monolayer surfactant intercalation. The extent of interdigitation is such that interactions between different chain methylenes are intense. The other organobentonites comprise bilayer intercalated surfactants with weaker interactions between different chain methylenes.

## **Conclusions**

Surfactants comprising one or two long alkyl chains were intercalated into bentonite in excess of the value equivalent to the CEC. The maximum amount intercalated of surfactants with single alkyl chains paralleled the chain length. In turn, surfactants with two alkyl chains were intercalated in similar amounts, essentially independent on the chain length.

XRD diffractometry, FTIR spectroscopy and thermogravimetric analysis were combined to probe the nature of the interlayer structures and its molecular environments. It has been concluded that samples SC12 and SC14 consist of monolayers of interdigitated surfactant configurations. The extent of interchain penetration caused strong hydrophobic interactions between different chain methylenes. The double chain C10, C16 and C18 alkyl surfactants intercalated as bilayers but XRD also hints at the presence of a minor phase comprising interdigitated surfactant configurations.

The onset decomposition temperature of present organobentonites, around 200 °C, is within the typical polymer/organoclay processing temperatures. The thermal stability of the present organobentonites was independent of both the number of alkyl chain substituents and their length.

## **Acknowledgements**

Financial support for this research from the Institutional Research Development Programme (IRDP) and the National Research Foundation (NRF) of South Africa is gratefully

acknowledged. We are also grateful for samples and technical support provided by G & W Base & Industrial Minerals. The first author also acknowledges the grace of God that inspired him in moments of darkness.

## References

- [1] Xi, Y., Martens, W., He, H., & Frost, R. (2005). *J. Therm. Anal. Calorim.*, 81, 91.
- [2] He, H., Ma, Y., Zhu, J., Yuan, P., & Qing, Y. (2010). *Appl. Clay Sci.*, 48, 67.
- [3] Xie, W., Gao, Z., Liu, K., Pan, W., Vaia, R., Hunter, D., & Singh, A. (2001). *Termochim. Acta* 367–368, 339.
- [4] Hang, P., & Brindley, G. (1970). *Clays Clay Miner.*, 18, 203.
- [5] Massinga Jr., P., Focke, W., de Vaal, P., & Atanasova, M. (2010). *Appl. Clay Sci.*, 49, 142.
- [6] Greene-Kelly, R. (1955). *Mineral. Mag.* 228.
- [7] Brown, G., & Brindley, G. (1980). *Crystal structure of clay minerals and their X-ray identification*, Mineralogical Society 5: London, UK.
- [8] Utracki, L. (2004). *Clay-containing polymeric nanocomposites*, Rapra Technology Limited: UK.
- [9] Lagaly, G. (1976). *Angew. Chem. Int. Ed. Engl.*, 15, 575.
- [10] Lagaly, G. (1986). *Solid State Ionics* 22, 43.
- [11] Vaia, R., Teukolsky, R. & Giannelis, E. (1994). *Chem. Mater.*, 6, 1017.
- [12] He, H., Frost, R., & Zhu, J. (2004). *Spectrochim. Acta A* 60, 2853.
- [13] He, H., Frost, R., Bostrom, T., Yuan, P., Duong, L., Yang, D., Xi, Y. & Klopogge, T. (2006). *Appl. Clay Sci.*, 31, 262.
- [14] Lagaly, G., & Weiss, A. (1970a). *Kolloid-Z. u. Z. Polym.*, 237, 364.
- [15] Lagaly, G., & Weiss, A. (1970b). *Kolloid-Z. u. Z. Polym.*, 238, 485.
- [16] Kopka, H., Beneke, K., & Lagaly, G. (1998). *J. Colloid Interf. Sci.*, 123, 427.

[17] Xi, Y., Ding, Z., He, H., & Frost, R. (2004). *J. Colloid Interf. Sci.*, 277, 116.

[18] Li, Z., & Jiang, W. (2009). *Thermochim. Acta* 483, 58.

## List of Tables

**Table 1.** Inorganic chemical composition (dry basis expressed as mass %) of clay samples before and after organic treatment

**Table 2.** XRD basal spacing values and FTIR  $\nu_{as}(\text{CH}_2)$  and  $\delta(\text{CH}_2)$  frequencies

**Table 3.** TGA mass loss and organic content intercalated.

## List of Figures

Fig. 1. XRD diffractograms of crude Koppies clay and organic derivatives

Fig. 2. TG curves of crude Koppies clay and organic derivatives

Fig. 3. DTG curves of crude Koppies clay and organic derivatives

**Table 1.** Inorganic chemical composition (dry basis expressed as mass %) of clay samples before and after organic treatment

	SiO <sub>2</sub>	Al <sub>2</sub> O <sub>3</sub>	Fe <sub>2</sub> O <sub>3</sub>	MgO	Na <sub>2</sub> O	CaO	K <sub>2</sub> O	P <sub>2</sub> O <sub>5</sub>	TiO <sub>2</sub>	MnO
<b>KP</b>	64.66	20.03	5.73	4.29	0.37	2.90	1.34	0.17	0.37	0.15
<b>SC14</b>	63.14	21.99	7.28	4.36	0.07	0.97	0.90	0.86	0.36	0.07
<b>SC16</b>	64.27	21.67	6.14	4.31	0.08	1.48	0.89	0.76	0.35	0.06
<b>DC16</b>	64.99	21.42	6.13	4.33	0.14	0.82	0.86	0.92	0.33	0.06
<b>DC18</b>	65.32	21.40	5.98	4.25	0.08	0.87	0.89	0.83	0.33	0.06

**Table 2.** XRD basal spacing values and FTIR  $\nu_{as}(\text{CH}_2)$  and  $\delta(\text{CH}_2)$  frequencies

Sample	XRD $d$ -spacing	Chain tilt angle <sup>1</sup>	FTIR $\nu_{as}(\text{CH}_2)$	FTIR $\delta(\text{CH}_2)$
	Nm	°	cm <sup>-1</sup>	cm <sup>-1</sup>
KP	1.52		-	-
SC12	1.92	29	-	-
SC14	1.84	22	2924	1476
DC10	2.66	23	2925	1469
DC16	3.82	32	2923	1468
DC18	3.88	29	2918	1469

<sup>1</sup>Estimated from equation (1) or equation (2)**Table 3.** TGA mass loss and organic content intercalated.

Sample	Mass loss, mass %		Organic content, mass %		
	150°C	1000°C	Theory <sup>2</sup>	Experimental	CEC
KS	18.9	17.7	-	-	-
SC12	97.9	72.2	16.2	21.2	1.31
SC14	95.4	68.4	17.9	23.3	1.30
DC10	96.5	62.6	21.7	30.6	1.41
DC16	97.4	50.8	31.0	44.2	1.43
DC18	97.2	50.1	31.9	44.9	1.41

<sup>2</sup>Based on the assumption of CEC level exchange

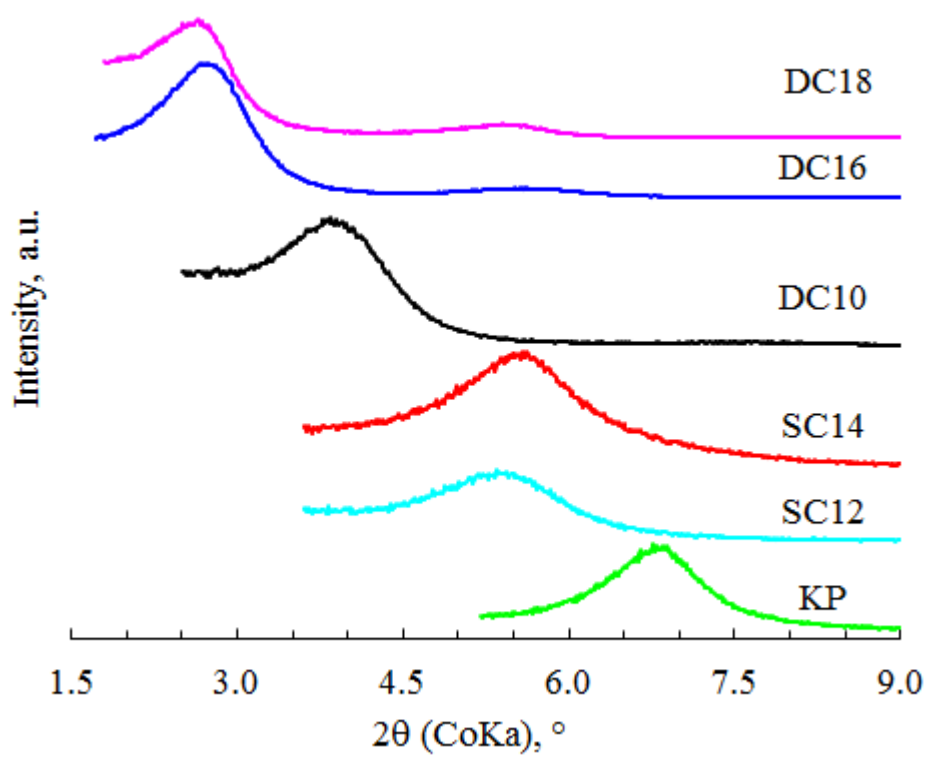


Fig. 1. XRD diffractograms of crude Koppies clay and organic derivatives

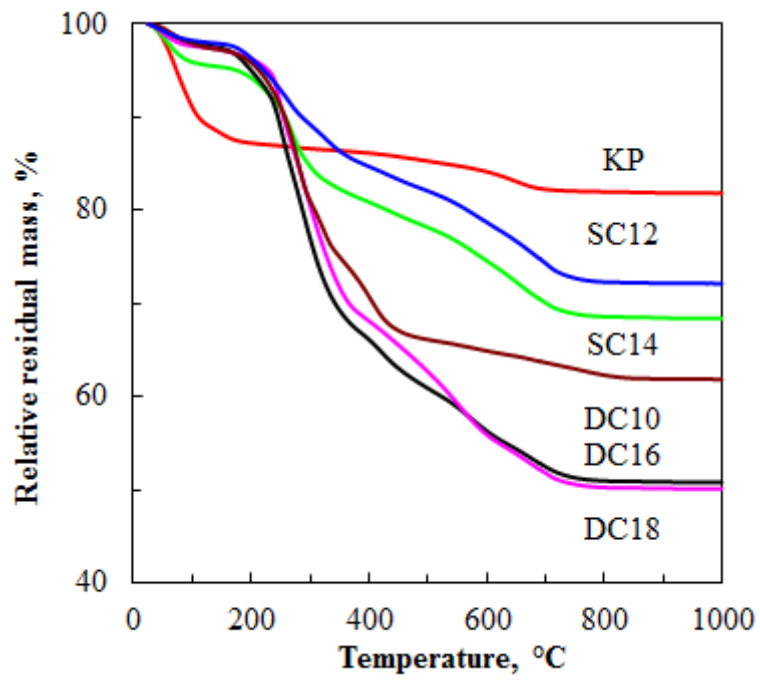


Fig. 2. TG curves of crude Koppies clay and organic derivatives

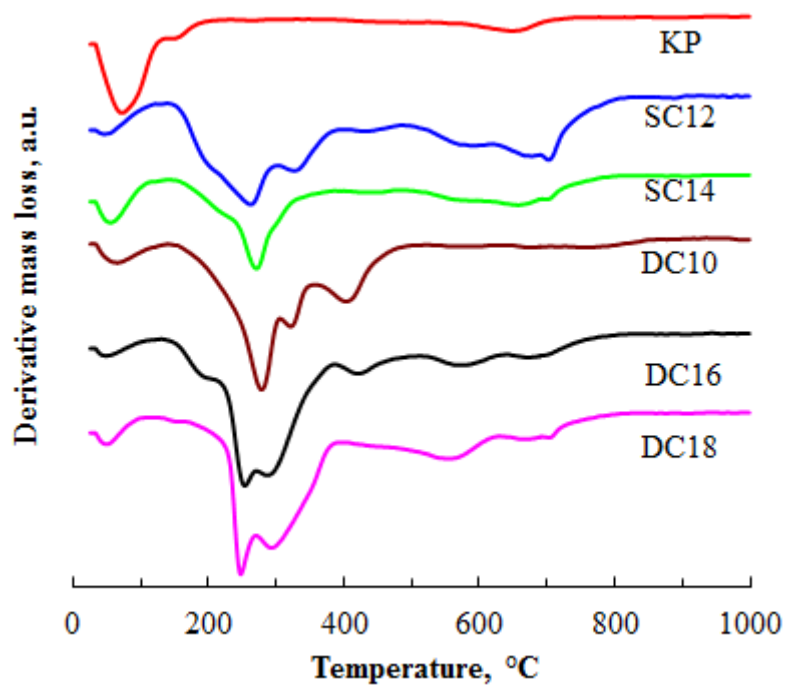


Fig. 3. DTG curves of crude Koppies clay and organic derivatives